frontiers in Ecology and Evolution

ORIGINAL RESEARCH
published: 21 July 2020
doi: 10.3389/fevo.2020.00209

Meristem Genes in the Highly Reduced Endoparasitic *Pilostyles boyacensis* (Apodanthaceae)

Angie D. González[1], Natalia Pabón-Mora[2], Juan F. Alzate[3,4] and Favio González[5]*

[1] Departamento de Biología, Facultad de Ciencias, Universidad Nacional de Colombia, Bogotá, Colombia, [2] Instituto de Biología, Universidad de Antioquia, Medellín, Colombia, [3] Centro Nacional de Secuenciación Genómica—CNSG, Sede de Investigación Universitaria—SIU, Universidad de Antioquia, Medellín, Colombia, [4] Grupo de Parasitología, Facultad de Medicina, Universidad de Antioquia, Medellín, Colombia, [5] Instituto de Ciencias Naturales, Facultad de Ciencias, Universidad Nacional de Colombia, Bogotá, Colombia

The family Apodanthaceae comprises two genera (*Apodanthes* and *Pilostyles*) and 11 endoparasitic species, all of them lacking root and shoot apical meristems, stems, and leaves. Their vegetative phase is reduced to a mycelium-like endophyte formed by strands of parenchyma cells that are in close contact to the host vasculature. These plants become apparent only when their tiny gregarious flowers emerge breaking through the host cortex. The lack of vegetative meristems in these plants sharply contrasts to the typical formation of floral meristems. Our target species, *Pilostyles boyacensis*, provides a suitable system to investigate the evolution of meristem-related genes in an endoparasitic flowering plant without a typical vegetative shoot apical meristem. We have generated transcriptomes from two different developmental stages of the parasite (emerged floral buds and fruits), as well as a mixed sample that comprises the endophyte and growing floral buds of the parasite and its host, *Dalea cuatrecasasii* (Fabaceae). We specifically assessed copy number and domain conservation for the *WUSCHEL HOMEOBOX*, *LRR-RLK-IX-a*, and *CLE* families related to the maintenance of the shoot apical meristem (SAM) as well as the *ARF* and *LFY* families responsible for floral meristem identity. Five out of the 11 canonical gene families responsible for SAM maintenance and floral fate determinacy targeted in this study were found in *Pilostyles*. *P. boyacensis* shows at least one transcript with all functional domains conserved for *BAM1*, *WUS*, *WOX9*, *ARF7*, and *LFY*. Other genes implicated in the canonical regulatory network could not be found, including *ARF5*, *ARF19*, *BAM2*, *BAM3*, *CLV1*, and *CLV3*. In conclusion, the endoparasitic lifestyle of Apodanthaceae appears to correlate with a substantial reduction in the transcriptomic machinery linked to SAMs, whereas the genes involved in flower fate have remained intact.

Keywords: ***AUXIN RESPONSE FACTOR 7*, *BARELY ANY MERISTEM*, *holoparasitic plants*, *LEAFY*, *shoot apical meristem*, *WUSCHEL***

Edited by:
Annette Becker, University of Giessen, Germany

Reviewed by:
Lachezar A. Nikolov, University of California, Los Angeles, United States
Luiza Teixeira-Costa, University of São Paulo, Brazil

****Correspondence:***
Natalia Pabón-Mora
lucia.pabon@udea.edu.co

Specialty section:
This article was submitted to Evolutionary Developmental Biology, a section of the journal Frontiers in Ecology and Evolution

Received: *15 January 2020*
Accepted: *08 June 2020*
Published: *21 July 2020*

Citation:
González AD, Pabón-Mora N, Alzate JF and González F (2020) Meristem Genes in the Highly Reduced Endoparasitic Pilostyles boyacensis (Apodanthaceae). Front. Ecol. Evol. 8:209. doi: 10.3389/fevo.2020.00209

INTRODUCTION

The basic body plan in vascular plants results essentially from the activity of two primary meristems that form roots [root apical meristem (RAM)] and shoots [shoot apical meristem (SAM)]. These meristems are established during early embryogenesis and are maintained during plant growth by complex genetic regulatory networks (Ha et al., 2010). In angiosperms, the SAM variously

forms phytomers with photosynthetic phyllomes before its transition to flowering. Several genes are known to control the shoot meristematic activity. In *Arabidopsis thaliana* the *WOX* family gene *WUSCHEL* (*WUS*) maintains the pluripotency and cell division rate (Gaillochet and Lohmann, 2015). In turn, this protein induces the production of the short peptide CLAVATA3 (CLV3, a member of the CLAVATA 3/ESR-related genes, the *CLE* family), which binds to the CLAVATA1 receptor (CLV1, subfamily *LEUCINE-RICH REPEAT RECEPTOR-LIKE KINASE IX-a, LRR-RLK-IX-a*), triggering the negative regulation of *WUS* and leading to cell differentiation at the periphery of the SAM (Gaillochet and Lohmann, 2015). This finely tuned feedback loop keeps a balance between cell division and differentiation and is reinforced by the action of the receptors BARELY ANY MERISTEM 1–3 (BAM1, BAM2, BAM3; members of the *LRR-RLK-IX-a*). BAM receptors are expressed in the periphery of the meristematic field, where they capture other peptides of the CLE family produced on the flanks and avoid complete differentiation of the meristematic cells by the effect of CLE peptides with CLAVATA1 (DeYoung and Clark, 2008). In addition, *WUSCHEL-HOMEOBOX 9* (*WOX9*, another member of the *WOX* family) has been shown to maintain active cell division in the SAM, leaf primordia initiation, and root meristem identity at early stages of seedling growth (Haecker et al., 2004; Wu et al., 2005). Thus, *wox9* mutants develop an abnormal flattened SAM with differentiated cells as well as the arrest of primary root growth (Wu et al., 2005). *WOX9* positively regulates *WUS* expression, and also responds to the negative regulation of CLV3 (Wu et al., 2005).

Hormones also play a key role in the patterning of the SAM. High concentrations of auxin on the SAM flanks are crucial for phyllome patterning, as auxin/indole-3-acetic acid (Aux/IAA) proteins interact with *AUXIN RESPONSE FACTOR 5* (*ARF5*/*MONOPTEROS*, a member of the *ARF* family) (Korasick et al., 2014). *ARF5* is repressed by IAA12/BODENLOS; such repression can be antagonized by high concentrations of auxin, triggering IAA protein degradation (Chandler, 2016). Thus, an increase of auxin in the flanks of the inflorescence meristem (IM) is necessary to release *ARF5,* which can directly induce *LEAFY* (*LFY*) and specify floral meristem (FM) fate (Yamaguchi et al., 2013; Denay et al., 2017). In addition, both *ARF5* and *ARF7* are functionally redundant in embryo axis patterning and auxin-dependent cell expansion (Hardtke et al., 2004). Furthermore, the closely related paralogs *ARF7* and *ARF19* could also induce *LFY* expression indirectly through the positive regulation of *PLETHORA3* (Chandler and Werr, 2015; Taylor-Teeples et al., 2016). *LFY* promotes the transcription of *APETALA1* (*AP1*) (Wagner et al., 1999) in a positive feedback loop responsible for FM identity. *LFY* containing complexes also activate B-, C- and E-class MADS-box genes, which ultimately control floral organ identity (Wils and Kaufmann, 2017).

Parasitic flowering plants have evolved independently at least 12 times (Nickrent, 2020). Hemiparasites are still able to photosynthesize and acquire water and minerals from its host plant. Holoparasites, instead, completely lack photosynthetic organs and relay on the host for all nutritional requirements. Such lifestyle is associated with variations of the typical body plan in response to full nutritional and developmental dependence on the host. The most dramatic reduction occurs in endoparasitic plants, which do not form roots, stems, or leaves (Heide-Jørgensen, 2008). Their vegetative phase is reduced to strands of parenchyma cells inside the host, and their only visible structures are the flowers and the fruits upon their emergence from the host tissues. Flowers frequently retain a variously modified perianth as well as a fully functional androecium and gynoecium (Heide-Jørgensen, 2008; Nikolov et al., 2013). Here, we focus on one of such extraordinary endoparasitic lineages, the Apodanthaceae. The family comprises 11 species in two genera, *Apodanthes* and *Pilostyles* (González and Pabón-Mora, 2014a,b). While the sole species of the former parasitizes members of the Salicaceae and is restricted to the New World, members of the latter grow on various legume lineages in the Americas, Africa, the Near East, and Australia (Bellot and Renner, 2014; González and Pabón-Mora, 2014a,b; Arias-Agudelo et al., 2019). Species of *Pilostyles* have a reduced embryo with 8–10 cells, and it is not known whether RAM or SAM formation occurs during early embryogenesis (Rutherford, 1970; González and Pabón-Mora, 2017; **Figure 1M**). The endophyte consists of mycelium-like cell strands in close contact with the host vasculature (**Figures 1H–J**). The reproductive transition occurs inside of the host passing through a bractless IM that quickly transitions into a FM. Flowers gradually break through the host cortex and emerge in preanthesis (Blarer et al., 2004; Brasil, 2010; Amaral and Ceccantini, 2011; González and Pabón-Mora, 2017; **Figures 1A–G**). Emerging portions are part of the exophyte (**Figures 1A–F**). The lack of recognizable vegetative meristems in these plants sharply contrasts to the typical formation of FMs, which poses a suitable system to study the evolution of meristem-related genes and the interplay between vegetative and FMs across flowering plants (**Figures 1K,L**).

Our study generates for the first time reference transcriptomes from three different developmental time points of the endoparasitic *Pilostyles boyacensis*, namely, endophytic tissue of *P. boyacensis* growing inside the *Dalea cuatrecasasii* host stem, individual floral buds, and fully formed fruits of *P. boyacensis*. We have identified a set of genes involved in shoot apical and FMs. We provide a comprehensive list of meristem-related genes in *Pilostyles* and track their evolution in a broad angiosperm sampling. Altogether, the substantial reduction of the SAM genetic regulatory network affects only the formation of primary meristems, while FM development remains intact. The few SAM meristematic genes found could be functionally recruited in flower, fruit, and early embryogenesis as indicated by their expression in the *P. boyacensis* flowers and fruits.

MATERIALS AND METHODS

Plant Material

Three samples spanning the full life cycle of the endoparasitic *P. boyacensis* were collected: (1) endophytic tissue of *P. boyacensis* growing inside the *D. cuatrecasasii* host stem (hereafter called PbE + D, **Figure 1G**); (2) individual preanthetic flowers of *P. boyacensis* already emerged from the host (hereafter called

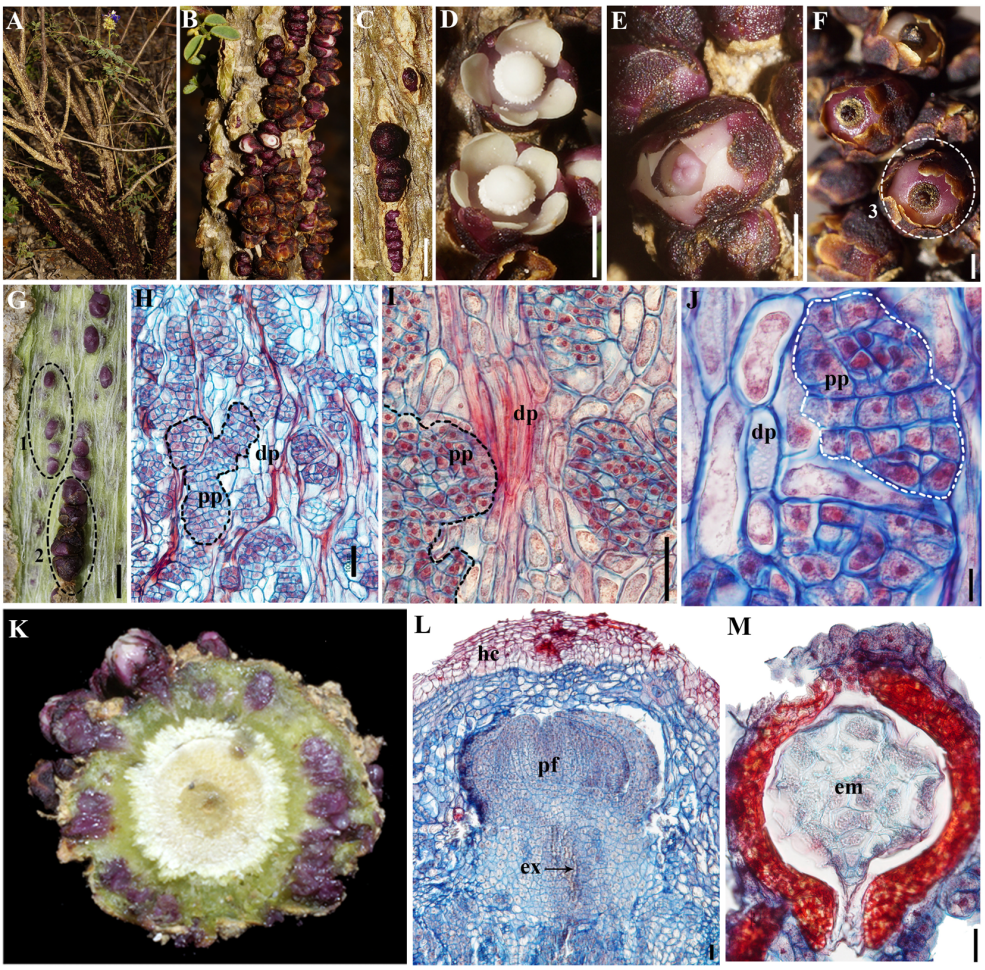

FIGURE 1 | (A–F) *Pilostyles boyacensis* exophyte; **(A–C)** overall view; **(A)** detail of flowers; **(B,C)** flowers emerging from its host *Dalea cuatrecasasii*. **(D)** Staminate flowers; **(E)** carpellate flowers; **(F)** fruits; **(G)** Peeled-off stem portion of *D. cuatrecasasii* showing flowers of *P. boyacensis* at various stages of development and growth; white fibers correspond to the phloem host tissue. **(H–J)** Longitudinal section of infected *D. cuatrecasasii* stem at **(H)** low; **(I)** mid and, **(J)** high magnification showing irregular aggregations of *Pilostyles* parenchymatic cells (pp, dotted) in contact to host phloem (dp). **(K)** Transverse section of infected *D. cuatrecasasii* stem showing flowers of *P. boyacensis* at various stages of development and growth; **(L)** Longitudinal section of *P. boyacensis* floral bud (pf) and its vascular extensor (ex), still inside of the host cortex (hc). **(M)** Longitudinal section of *P. boyacensis* seed with embryo (em). Numbers (1–3) in **(F)** and **(G)** indicate the three tissues sampled for the transcriptomes, as follows: (1) *Dalea*/*Pilostyles* mixed tissue; (2) Preanthetic *Pilostyles* flowers; (3) *Pilostyles* fruits and seeds. Scale bars: **(C–G)** 2 mm; **(H,I,L)** 100 μm; **(J)** 10 μm; **(M)** 20 μm.

PbFl, **Figure 1** G); and (3) young and fully formed fruits and seeds of *P. boyacensis* (hereafter called PbFr, **Figure 1F**). These samples were collected at xerophytic thickets around Villa de Leyva (Boyacá, Colombia) for total RNA extraction (*Pilostyles* voucher *FG 4518*, and *D. cuatrecasasii* voucher *FG 4519*, both deposited at COL). The tissues were flash-frozen in the field and stored in liquid nitrogen until RNA extraction was performed.

RNA Extraction, Sequencing, and Transcriptome Assembly

The TRIzol™ Reagent (Invitrogen) protocol was used for the extraction of total RNA with modifications used by Pabón-Mora et al. (2012). Total RNA was resuspended in 1 ml of EtOH 100% and send out to the Macrogen Sequencing Facility. The RNA-seq experiment was conducted using the Truseq mRNA library construction kit (Illumina) and sequenced on a HiSeq2000 instrument[1]. Read cleaning was performed with a quality threshold of Q30, and a minimum read length of 70 bp, singletons were excluded. Contig assembly was computed using the Trinity V2.5.1 software (Grabherr et al., 2011) with default settings with TRIMMOMATIC adapter removal. Assemblage metrics are summarized in **Table 1**.

Identification of Orthologous Genes Associated With the Regulation of Shoot Apical and Floral Meristems

The canonical genes *ARF5*, *ARF7*, *ARF19*, *BAM1*, *BAM2*, *BAM3*, *CLV1*, *CLV3*, *LFY*, *WOX9*, and *WUS*, involved in the SAM

[1]https://www.illumina.com/

TABLE 1 | Statistics of the PbE + D, PbFl, and PbFr transcriptomes.

	PbE + D	PbFl	PbFr
Number of paired raw reads	72535272	50851360	64546194
Number of contigs	321853	177935	147327
Average contig length	644	592	867
Largest contig	12072	16382	13560
Shortest contig	201	201	201
N50	1009	850	1554
L50	57252	29037	24532
GC%	43.88	42.07	43.5

maintenance and FM fate in *Arabidopsis thaliana*, were retrieved from TAIR (The Arabidopsis Information Resource, Poole, 2007). Then, they were used as queries to search homologs in the transcriptome of *Pilostyles thurberi* (available in the OneKP database; Matasci et al., 2014) as well as in other members of the Cucurbitales, including the genomes of *Cucumis sativus* (available in Phytozome; Goodstein et al., 2012), *Citrullus lanatus* and *Cucurbita maxima* (available in Cucurbit Genomics Database; Zheng et al., 2019). These sequences were compiled and processed to keep exclusively their coding sequences (CDS). A complete matrix for each gene lineage was used as query in the transcriptomes from *P. boyacensis* and *D. cuatrecasasii* described above. BLAST searches were done using an *e*-value of 1×10^{-5} and 1×10^{-30}. *P. boyacensis* genes isolated have been submitted to NCBI under the GenBank numbers MN946521–MN946537.

Sequences resulting from the search in the three *Pilostyles* transcriptomes were then subjected to BLASTN in NCBI. Two searches were performed in order to identify the best hits from the database and to assess their preliminary taxonomic affinity. The first search was done without any taxonomic filters. Here, all *Pilostyles* sequences used as queries resulted in high identity hits with genes from several taxa in the Malpighiales. The second search was done taking into consideration particular taxonomic filters, thus providing the framework to preliminary assign each sequence to either *P. boyacensis* or *D. cuatrecasasii*. This is particularly important for those sequences obtained from the mixed host-parasite transcriptome. Genes were preliminarily assigned to *P. boyacensis* when BLAST searches resulted in high identity and coverage values with sequences from members of Cucurbitales (where Apodanthaceae is currently circumscribed) and Malpighiales (where the first search yielded most hits). On the other hand, genes were assigned to *D. cuatrecasasii* if best hits matched sequences from Fabaceae (as host-related proxies). BLAST searches in Swiss-Prot (sub-base plants) were used to determine whether the sequences extracted corresponded to the target gene.

Characterization of Orthologous Genes Associated With the Regulation of Shoot Apical and Floral Meristems

In order to explore the evolution of the target genes, five independent matrices were compiled for the *ARF5*/*7*/*19*, *CLV1*/*BAMs, LFY*, *WOX9*, and *WUS* genes. These matrices included all sequences isolated from the three reference transcriptomes described above, as well as canonical sequences from *A. thaliana*, and other selected basal angiosperms, monocots, rosids, and asterids. These sequences were extracted from the GenBank, Hardwood Genomics Project[2] Phytozome and OneKP. The CDSs were identified using TransDecoder[3] implemented on the Galaxy platform (Afgan et al., 2018). The complete accession list is in **Supplementary Table S1**.

Sequences were compiled using Bioedit (Hall, 1999) and aligned in two steps: a first, unguided alignment followed by a phylogenetic analysis in order to identify major clades within large gene families such as ARF, BAM, and CLV; and a second, refined alignment guided by sequence similarity found among closely related taxonomic groups for each gene family. Alignments were made using the MAFFT server (Katoh and Standley, 2013) implementing the E-INS-I strategy, a gap opening penalty of -2 and an offset of 0.5 for most genes, except for *WUS* and *WOX9*, where a gap opening value of −3 was used. For the second alignment phase, the merge function of MAFFT was used to compile smaller datasets into a single matrix per gene family[4].

In order to find the evolutionary model that best fits each matrix, ModelTest-NG (Darriba et al., 2019) was used, resulting in the GTR + G model for all gene families. Phylogenetic analyses were carried out by two approaches. First, maximum likelihood using RaxML-HPC2 (Stamatakis et al., 2008) with 500–1000 bootstrap and all other parameters by default. Second, Bayesian inference was applied using MrBayes 3.2.7a (Ronquist et al., 2012) with two independent runs with four chains, convergence between runs assessed by average standard deviation of split frequencies below 0.01, and burn-in of 25% to obtain a majority-rule consensus tree. Some features were adjusted for each gene lineage, as follows: for *WUS* and *WOX9*, three million generations were run with a sample frequency of 500; for *LFY*, six million generations were run with a sample frequency of 500; for *CLV1*/*BAMs*, 30 million generations were run with a sample frequency of 3,000; and for *ARF5*/*7*/*19*, eight million generations were run with a sample frequency of 250. The *Amborella trichopoda* homologs were chosen as outgroup in most phylogenetic analyses with two exceptions; the *A. thaliana PHLOEM INTERCALATED WITH XYLEM* (*PXY*) was used as outgroup in the *LRR-RLK-IX-a* family, given that it predates the *CLV*/*BAM* duplication (Bryan et al., 2012); and the *Physcomitrella patens ARF2* was used as outgroup in the *ARF5/7/19* family, as it precedes the split of *ARF5* and *ARF7*/*19* (Finet et al., 2013). Software used for the evolutionary model search, maximum likelihood and Bayesian inference were run on the CIPRES Science Gateway (Miller et al., 2010). Resulting trees were visualized and edited using FigTree v. 1.4 (Rambaut, 2006).

Unaligned aminoacidic matrices generated in Bioedit (Hall, 1999) were used to search motifs in the MEME

[2]https://www.hardwoodgenomics.org

[3]https://github.com/TransDecoder/TransDecoder/wiki

[4]https://mafft.cbrc.jp/alignment/server/merge.html

Suite program[5] with the following parameters: Motif Site Distribution: zero or one per sequence; maximum number of motifs: 50; minimum motif width: 7; maximum motif width: 150, and all other default parameters. Selected sequences including those from *Pilostyles boyacensis*, *P. thurberi*, *A. thaliana*, Cucurbitaceae, Salicaceae, Euphorbiaceae, and Fabaceae were subjected to MEME analysis aiming to identify domains and motifs exclusive to Apodanthaceae. *A. thaliana* sequences were included in order to compare the canonical domains reported for those genes. Cucurbitales sequences were included as Apodanthaceae is currently a member of this order. Finally, Salicaceae and Euphorbiaceae (Malpighiales) proteins were included due to high similarity in the BLAST hits with *Pilostyles* sequences. Expanded complete (in the case of WUS, WOX9, and LFY) or partial (for CLV/BAM and ARF5/7/19) datasets of the amino acid matrices were analyzed by MEME to confirm Apodanthaceae exclusive motifs.

RESULTS

Pilostyles boyacensis orthologs of *ARF7, BAM1, LFY,* and *WOX9* were identified from all three transcriptomes. The *WUS* ortholog was found only in the PbFl transcriptome. Orthologs of *ARF5*, *ARF19, BAM2, BAM3, CLV1, CLV3* were not found in any of the three transcriptomes (**Table 2**). *CLE22* and *CLE3*, both of which are *CLE* homologs, were only found in the PbE + D transcriptome. Their CDS size ranges between 288 and 335 nt, and they likely belong to *D. cuatrecasasii*, as both sequences show high identities (70–82%) and coverages (98–100%) with various Fabaceae homologs.

[5]http://meme-suite.org/tools/meme

TABLE 2 | BLAST targeted genes in the three transcriptomes of *P. boyacensis* examined.

Gene family	Gene	PbE + D	PbFl	PbFr
WUSCHEL-related homebox (WOX)	*WUS*	–	*PiboW1* PiboW2*	–
	WOX9	*PiboW9_2*	*PiboW9_1** *PiboW9_2* *PiboW9_3*	*PiboW9_2*
CLAVATA 3/ESR-related (CLE)	*CLV3*	–	–	–
LEUCINE-RICH REPEAT RECEPTOR-LIKE KINASE IX-a, (LRR-RLK-IX-a)	*CLV1*	–	–	–
	BAM1	*PiboBAM1_1*	*PiboBAM2_1*	*PiboBAM1_2** *PiboBAM2_2** *PiboBAM2_3**
	BAM2	–	–	–
	BAM3	–	–	–
AUXIN RESPONSE FACTOR (ARF)	*ARF5*	–	–	–
	ARF7	*PiboARF7_2**	*PiboARF7_1** *PiboARF7_2**	*PiboARF7_2** *PiboARF7_3** *PiboARF7_4**
	ARF19	–	–	–
LEAFY	*LFY*	*PiboLFY3***	*PiboLFY1* *PiboLFY2*	*PiboLFY1* *PiboLFY2*

Single asterisks (*) indicate protein sequences lacking one or more motifs when compared to canonical proteins. Double asterisk (**) indicates incomplete CDS. (–): transcript not found.

The *WUSCHEL* and *WUSCHEL*-Related Homeobox 9 Gene Subfamilies

The phylogenetic reconstruction of the *WUS* genes is mostly consistent with the systematic relationships of the angiosperm groups sampled. The only exception is the odd position of monocot homologs within rosids, likely due to long-branch attraction or convergent sites. Rosid homologs are grouped by family; thus, gene clades from Apodanthaceae, Brassicaceae, Cucurbitaceae, Euphorbiaceae, Fabaceae, Linaceae, Malvaceae, and Salicaceae are recovered (**Figure 2**). *WUS* homologs are mostly single copy genes, except for the duplicates found in *Argemone mexicana* (Papaveraceae), *Cucurbita maxima* (Cucurbitaceae), *Gossypium raimondii* (Malvaceae), *Juglans regia* (Juglandaceae), *Linum usitatissimum* (Linaceae), and *Populus trichocarpa* and *Salix purpurea* (Salicaceae) (**Figure 2** and **Supplementary Figure S1**). Most duplicates appear to be species-specific, except in Salicaceae where the duplication predates the *Populus/Salix* diversification (**Figure 2**).

The two *Pilostyles boyacensis WUSCHEL (WUS)* homologs are closely related to the single sequence recovered from *P. thurberi* (bootstrap/posterior probability BS/PP, 100/1). *WUS* homologs from both *Pilostyles* species are, in turn, clustered with sequences from *Citrullus lanatus*, *Cucumis sativus*, and *Cucurbita maxima* (Cucurbitaceae) (BS/PP, 85/1, **Figure 2**).

The two contigs found in *P. boyacensis* were recovered from the PbFl transcriptome. These two differ in 10 bases and a four-base insertion that extends the reading frame by 38 amino acids toward the 3′ in one of the variants (PiboW2; **Supplementary Figure S2**). The MEME analysis shows that the Homeobox domain (DNA-binding domain), the LELxL WUS motif, and the TLxLFP WOX1 motif are conserved in PiboW2, while PiboW1 lacks the LELxL WUS motif (**Figure 3** and **Table 2**). The single transcript found in the transcriptome of *P. thurberi* shows a premature stop codon and only conserves the Homeobox domain. Our MEME analyses did not identify additional motifs exclusive for Apodanthaceae or Cucurbitaceae.

The phylogeny of the *WUSCHEL-related homeobox 9* genes recovers the monocot and the eudicot homologs with high supports (BS/PP, 86/0.98, and 70/1, respectively). However, the expected relationships within eudicot homologs are not recovered (**Figure 4**). Family-specific duplications were detected in Brassicaceae, resulting in the *WOX8* and *WOX9* clades, as well as in Crassulaceae, Poaceae and Salicaceae (**Figure 4** and **Supplementary Figure S3**). Species-specific duplications were detected in *Cucurbita maxima*, *Gossypium raimondii*, *Juglans regia*, *Linum usitatissimum*, *Musa acuminata*, *Pilostyles boyacensis, P.*

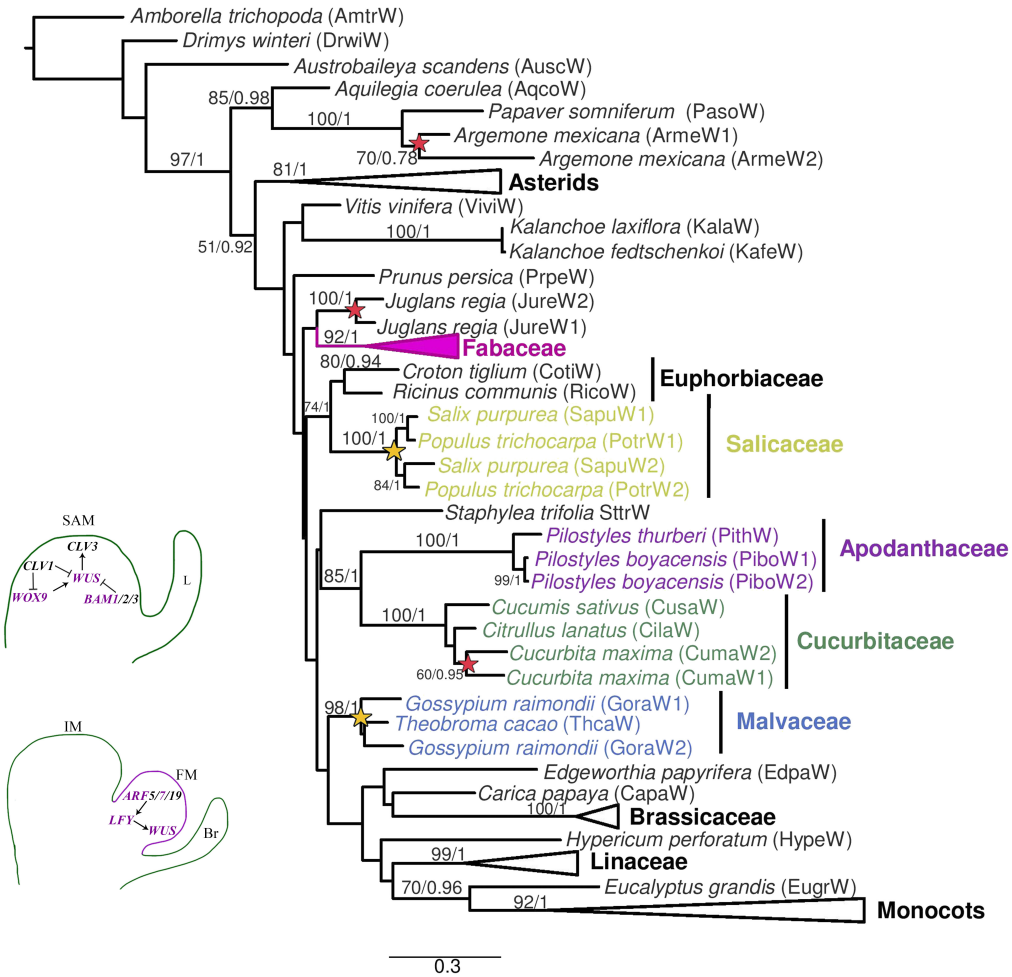

FIGURE 2 | Maximum likelihood reconstruction of the *WUSCHEL* gene lineage. Bootstrap values >50 and posterior probability are shown above the nodes. Yellow stars and red stars indicate family level and species-specific duplication events, respectively. Bottom left, schematic representation of the canonical genes related to the SAM and the transition to IM and FM. Abbreviations: *ARF, AUXIN RECEPTOR FACTOR; BAM, BARELY ANY MERISTEM;* Br, bract; *CLV, CLAVATA;* L, leaf; *LFY, LEAFY; WOX, WUSCHEL HOMEOBOX; WUS, WUSCHEL*.

thurberi, Phaseolus vulgaris, and *Staphylea trifolia* (**Figure 4** and **Supplementary Figure S3**).

All *Pilostyles* homologs cluster with Cucurbitaceae *WOX 9* genes in both phylogenetic reconstructions (BS/PP, 39/0.99, **Supplementary Figure S3**). In the case of *P. boyacensis*, three variants of *PiboWOX9* were detected, all of which were close to one of the two copies found in *P. thurberi* (*PithW9*_1, BS/PP, 100/1, **Figure 4**). The *PiboW9*_2 variant was found in all three transcriptomes, whereas the other two variants where only isolated from the PbFl transcriptome of *P. boyacensis*. The MEME analysis showed an N-terminal motif MASSN, the Homeobox domain, and the C-terminal VFIN/LQxG WOX8 motif, present in all sequences. The only exception was detected in the *PiboW9*_1 variant, which lacks the C-terminal VFIN/LQxG WOX8 motif (**Supplementary Figure S4**; **Table 2**). Two Apodanthaceae-specific motifs and one Cucurbitaceae-specific motif (**Supplementary Figure S4**) were found in a dataset that included 88 representative sequences from *A. thaliana*, Apodanthaceae, Cucurbitaceae, Salicaceae, and Euphorbiaceae (data not shown).

The LEUCINE-RICH REPEAT RECEPTOR-LIKE KINASE IX-a Subfamily

The phylogenetic reconstruction of the LRR-RLK-IX-a subfamily recovered four large clades *CLV1* (BS/PP, 84/0.67), *BAM1*/2 (BS/PP, 16/-), *BAM3* (BS/PP, 88/1), and *BAM3-like* (BS/PP, 65/1) (**Figure 5** and **Supplementary Figure S5**). *Amborella trichopoda* and species of Ranunculales have homologs in each of the four clades, suggesting that duplications occurred prior to the diversification of all angiosperms. However, in 49 out of 74 species, we only detected genes from two or three clades, pointing to heterogeneous expression of the four genes in different taxa. The maximum likelihood (ML) reconstruction of *CLAVATA1* subclade is mostly consistent with the phylogenetic relationships of the angiosperm groups sampled, as the *A. trichopoda CLV1* homolog clusters with the sampled genes from basal eudicots,

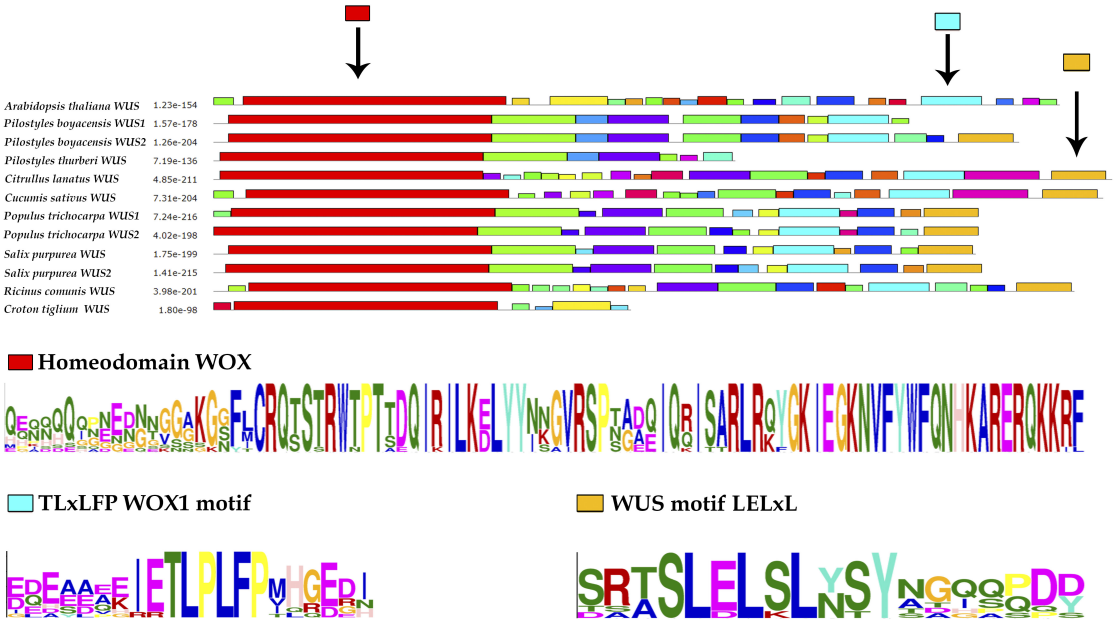

FIGURE 3 | MEME analysis of WUSCHEL proteins of *A. thaliana*, Apodanthaceae, Cucurbitaceae, Salicaceae, and Euphorbiaceae.

and asterid homologs separate from rosid genes (**Supplementary Figure S5**). The *CLV1* representatives from Brassicaceae, Cucurbitaceae, Euphorbiaceae, Fabaceae, Linaceae, Malvaceae, and Salicaceae form well-supported clades (**Supplementary Figure S5**). Local duplications of *CLV1* were detected in the host *Dalea cuatrecasasii*, as well as in *Gossypium raimondii, Kalanchoe laxiflora*, *Linum usitatissimum, Prunus persica*, and Salicaceae.

The clade formed by *BAM3* and *BAM3*-like was retrieved in both analyses (BS/PP, 67/1). The *BAM3*-like subclade includes sequences from *Amborella trichopoda*, representative monocots (*Musa acuminata*) and basal eudicots (Ranunculales; **Supplementary Figure S5**). Asterid and rosid homologs form two separate clades; within the latter, we recovered five variants from the PbE + D transcriptome assigned using BLAST to *Dalea cuatrecasasii* (**Supplementary Figure S5**). The *BAM3* phylogenetic reconstruction mirrors the taxonomic relationships among the angiosperm groups sampled (**Supplementary Figure S5**). The *BAM3* subclade recovers family-level duplications in Fabaceae and Salicaceae, as well as species-specific duplications in *Atropa belladonna, Brassica rapa*, *D. cuatrecasasii*, and *Linum usitatissimum* (**Supplementary Figure S5**).

The ML reconstruction of *BAM1*/2 genes includes sampling from gymnosperms and angiosperms, and like in previous analyses, it is consistent to the phylogenetic relationships of the taxa sampled, with the exception of the position of the monocot genes close to *Eucalyptus grandis* (Myrtaceae) sequences (**Figure 5**). Within eudicots, most asterid genes cluster together (BS/PP, 97/0.94). Family-level duplications are recovered in Apodanthaceae (BAM1/2), Brassicaceae (BAM1/2), Linaceae, Papaveraceae, and Poaceae. Species-specific duplications were detected in *Amaranthus hypochondriacus*, *Begonia* sp., *Chenopodium quinoa, Cladrastis lutea, Cucurbita maxima, Digitalis purpurea, Gossypium raimondii, Linum usitatissimum*, *L. perenne*, *Lonicera japonica, Medicago truncatula, Orobanche fasciculata*, and *Staphylea trifolia* (**Supplementary Figure S5**). Species from Salicaceae and Euphorbiaceae show only one copy of *BAM1/2* (**Supplementary Figure S5**). Apodanthaceae homologs are sisters to gene representatives from Salicaceae, Euphorbiaceae, and Linaceae, but support values are low (BS/PP, 35/0.67, **Supplementary Figure S5**). *BAM1/2* homologs from *P. boyacensis* clustered together with those from *P. thurberi* (BS/PP, 100/1, **Figure 5**).

The MEME analysis for selected sequences within the *BAM1*/2 gene clade detected four leucine-rich regions, two of which were identified using Pfam as LRR4 and LRR8 (both corresponding to the extracellular domain). Additionally, two motifs matched the kinase domains (corresponding to the cytoplasmic domain). The *P. boyacensis PiboBAM1_2*, *PiboBAM2_2*, *PiboBAM2_3* from PbFr, and the *C. sativus CusaBAM1.1* variants lack half of the protein kinase domain (**Supplementary Figure S6**; **Table 2**). Nevertheless, *PiboBAM1_1* isolated from PbE + D, and *PiboBAM2_1*identified in the PbFl transcriptome, as well as *CusaBAM1.2*, exhibit complete domains (**Supplementary Figure S6**; **Table 2**). No motifs exclusive for Apodanthaceae, Cucurbitaceae, or Cucurbitales were found.

The *AUXIN RESPONSE FACTOR 7* Gene Family

The phylogenetic reconstruction of the ARF5/7/19 gene lineages recovers five clades corresponding to *ARF7-A* (BS/PP, 99/1), *ARF7-B* (BS/PP, 61/0.99), *ARF5* (BS/PP, 68/0.88), *ARF7/19-D* (BS/PP, 97/1), and *ARF7-E* (BS/PP, 92/1,

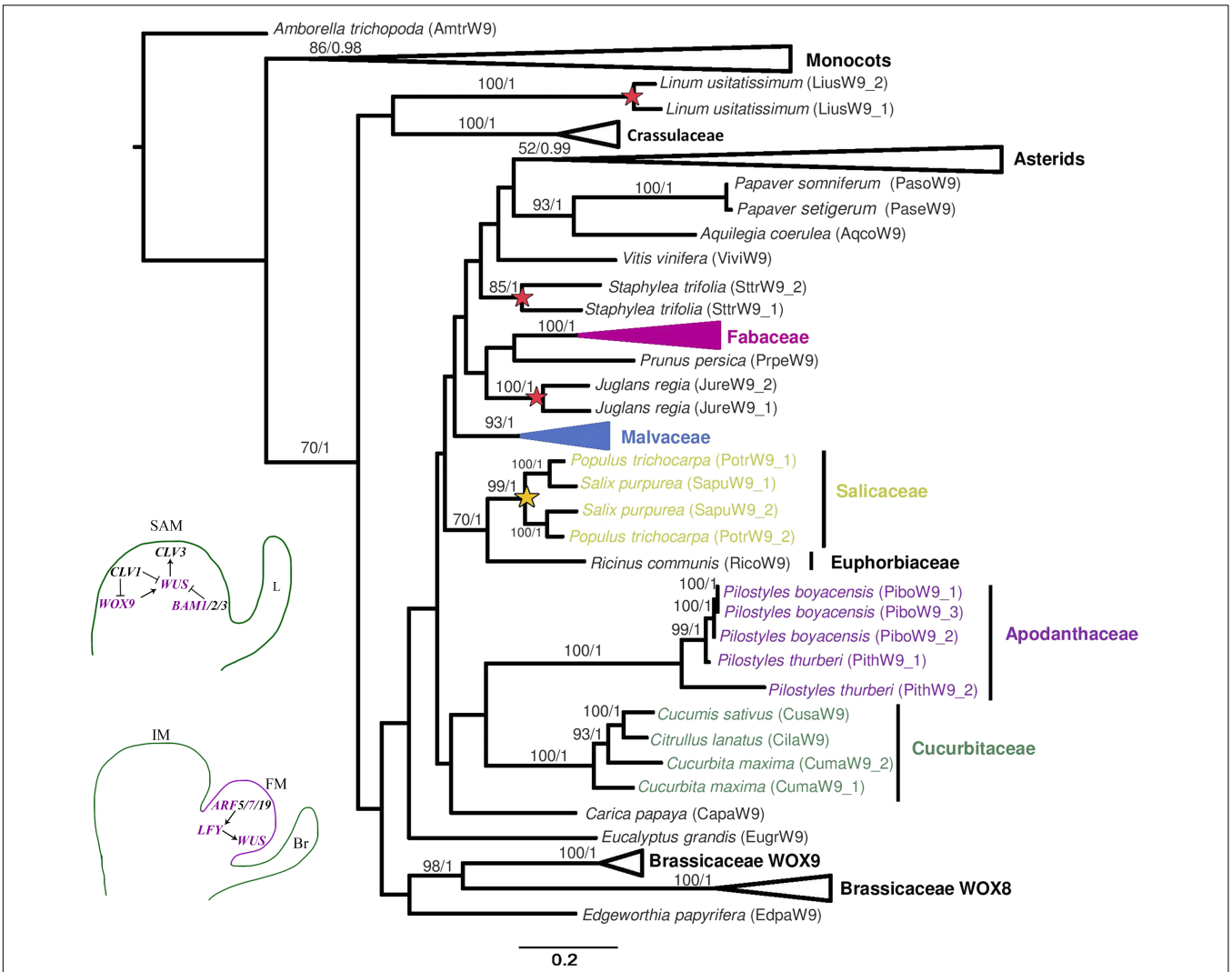

FIGURE 4 | Maximum likelihood reconstruction of the *WUSCHEL-HOMEOBOX 9* gene lineage. Bootstrap values >50 and posterior probability are shown above the nodes. Yellow stars and red stars indicate family-level and species-specific duplication events, respectively. Schemes in the bottom left follow the conventions in **Figure 2**.

Figure 6). The *Amborella trichopoda* and the *Austrobaileya scandens* homologs are found in four and three of the five clades, respectively (**Supplementary Figure S7**). This suggests that duplications occurred before the radiation of all angiosperms. Both *ARF7-A* and *ARF7-B* gene phylogenies are consistent with the phylogenetic relationships of the taxa sampled. Within *ARF7-A* no family-level duplications are detected. Only species-specific duplications are found in *Argemone mexicana, Linum perenne*, *Orobanche fasciculata*, *Papaver somniferum*, and *Papaver setigerum* (**Supplementary Figure S7**).

Within *ARF7-B* a large-scale duplication likely occurred in core eudicots because there are two clades recovered containing asterid and rosid (Salicaceae and Malvaceae) representatives. However, one of the two clades also includes homologs from Brassicaceae, Fabaceae, and Cucurbitaceae. In addition, species-specific duplications are found in *Argemone mexicana, Austrobaileya scandens, Castanea pumila, Gossypium raymondii, Lonicera japonica*, *Musa acuminata, Orobanche fasciculata, Papaver setigerum*, and *Papaver somniferum* (**Supplementary Figure S7**).

The *ARF5* clade has remained largely as a single copy, with no large-scale or family-level duplications (**Supplementary Figure S7**). Thus, well-supported gene clades are recovered for the *ARF5* homologs in Amaranthaceae, Brassicaceae, Euphorbiaceae, Fabaceae, Linaceae, Malvaceae, Orobanchaceae, Papaveraceae, Poaceae, Salicaceae, and Solanaceae (**Supplementary Figure S7**). Species-specific duplications are found only in *Amaranthus hypochondriacus, Conopholis americana, Gossypium raimondii, Mimulus guttatus, Musa acuminata*, and *Orobanche fasciculata* (**Supplementary Figure S7**).

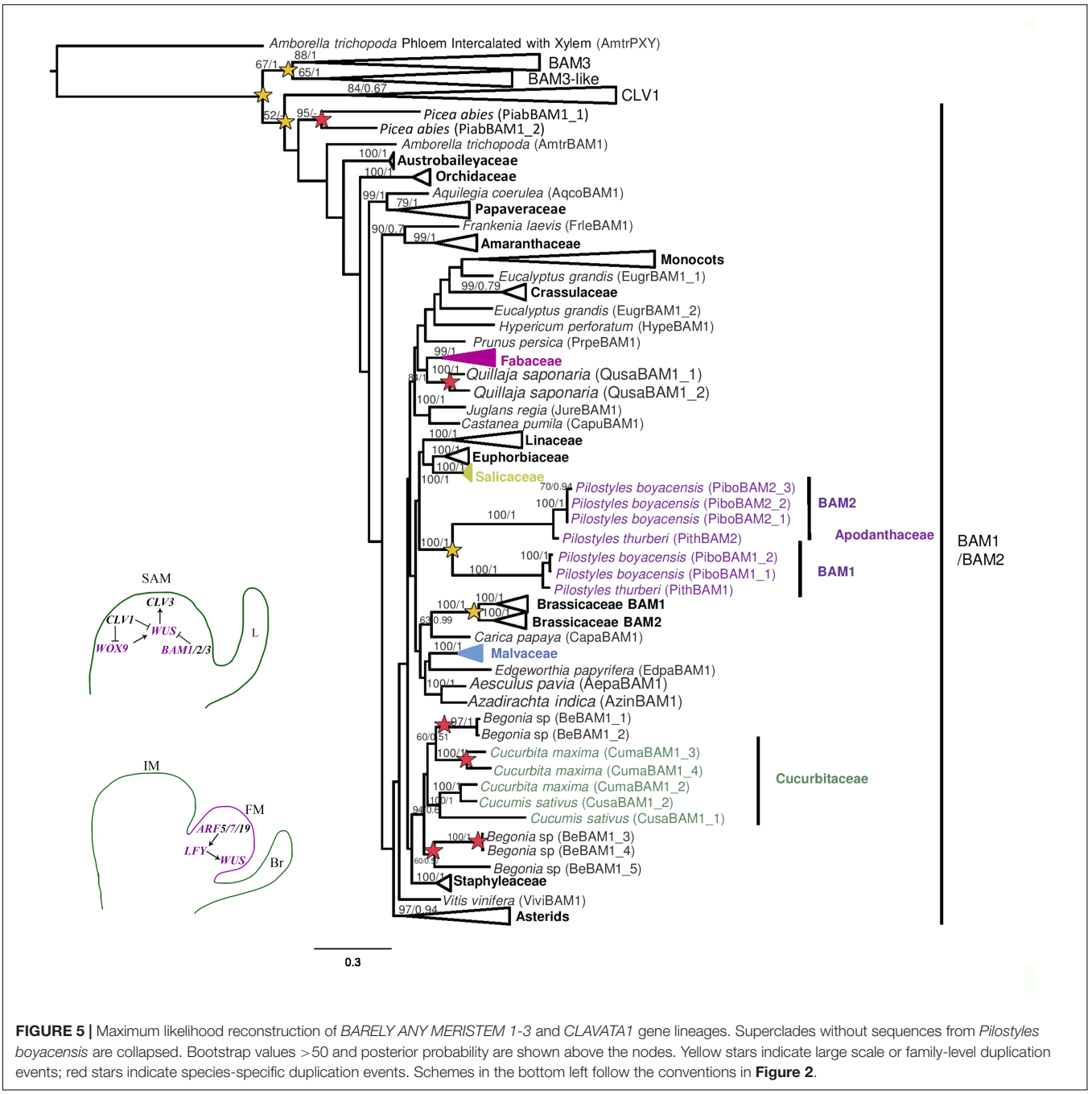

FIGURE 5 | Maximum likelihood reconstruction of *BARELY ANY MERISTEM 1-3* and *CLAVATA1* gene lineages. Superclades without sequences from *Pilostyles boyacensis* are collapsed. Bootstrap values >50 and posterior probability are shown above the nodes. Yellow stars indicate large scale or family-level duplication events; red stars indicate species-specific duplication events. Schemes in the bottom left follow the conventions in **Figure 2**.

In the *ARF7-D* clade, two family-level duplications can be detected, one in the Brassicaceae resulting in the *ARF7* and *ARF19* subclades and a second one within Fabaceae. The remaining *ARF7-D* homologs are retained as single copy except in *Amaranthus hypochondriacus, Argemone mexicana, Atropa belladonna, Castanea pumila, Edgeworthia papyrifera, Gossypium raimondi, Hypericum perforatum, Juglans regia, Linum perenne, Mimulus guttatus,* and *Papaver somniferum* (**Supplementary Figure S7**).

Finally, in the *ARF7-E* clade, family-level duplications were detected in Poaceae and Solanaceae, but most other homologs remain as single copy. Species-specific duplications were found in *Argemone mexicana, Conopholis americana, Hypericum perforatum, Linum perenne, L. usitatissimum, Musa acuminata, Papaver setigerum, P. somniferum, Salix purpurea*, and *Staphylea trifolia* (**Supplementary Figure S7**). In this clade, four variants were isolated from *Pilostyles boyacensis*. *PiboARF7*_2 was found in all three transcriptomes (PbE + D, PbFl, and PbFr), while the variant *PiboARF7*_1 is only found in the PbFl transcriptome, and variants *PiboARF7*_3 and *PiboARF7*_4 were isolated from the PbFr transcriptome. The four *P. boyacensis* and the

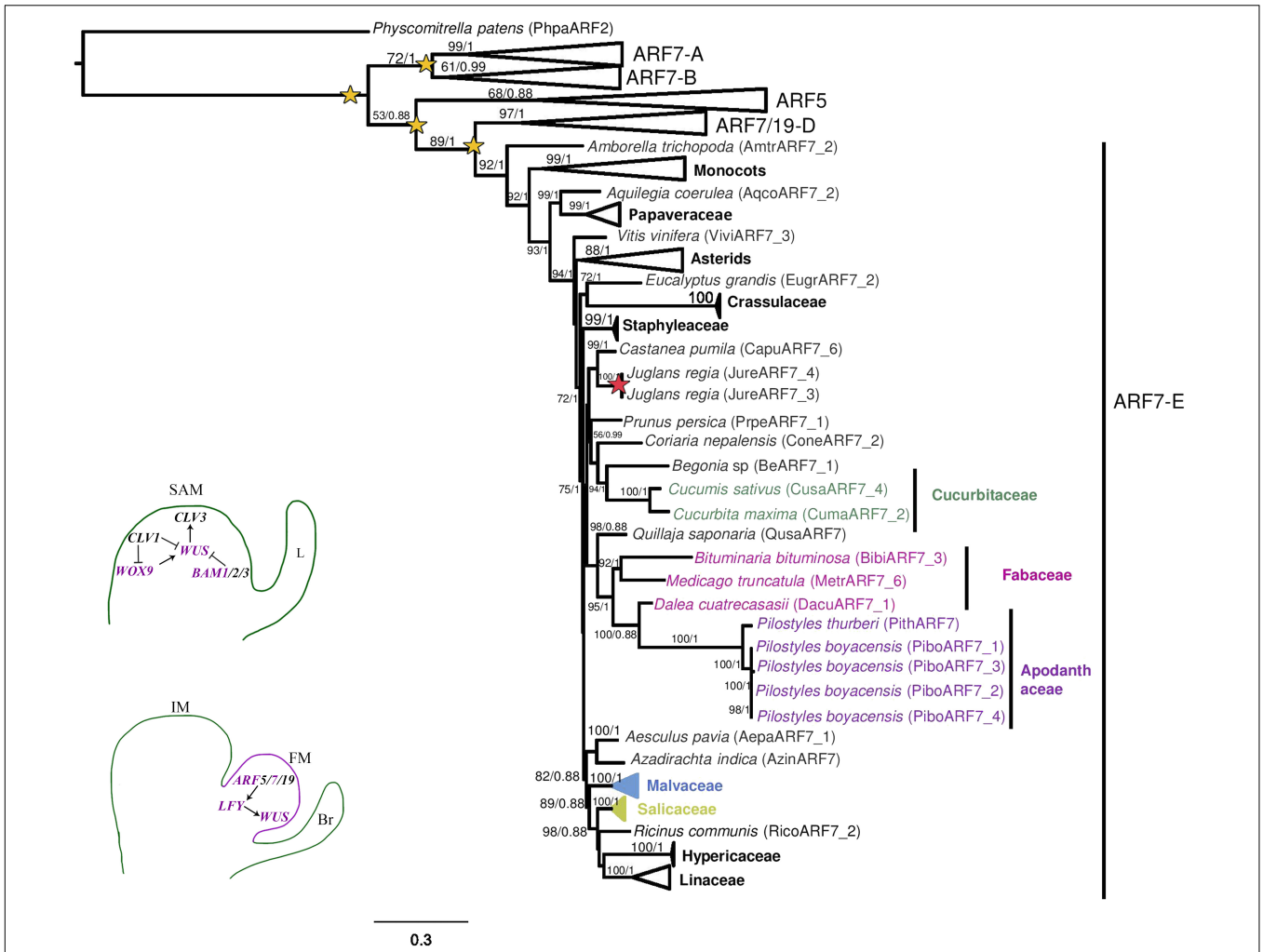

FIGURE 6 | Maximum likelihood reconstruction of the *AUXIN RESPONSE FACTOR 5/7/19* gene lineage. Superclades without sequences from *Pilostyles boyacensis* are collapsed. Bootstrap values >50 and posterior probability are shown above the nodes. Yellow stars indicate large scale or family-level duplication events; red stars indicate species-specific duplication events. Schemes in the bottom left follow the conventions in **Figure 2**.

single *P. thurberi* homologs clustered together (BS/PP, 100/1). The BLASTN comparison showed a similarity percentage of 78% and coverage of 55–74% with homologs from Euphorbiaceae and Salicaceae. Additionally, an *ARF7* homolog isolated from the PbE + D transcriptome, showing an identity of 85% and coverage of 98% with other species of Fabaceae, was assigned here to the host *D. cuatrecasasii* and labeled as *DacuARF7_1* (**Figure 6** and **Supplementary Figure S7**).

The MEME analysis detected the N-terminal B3 DNA binding and the Auxin response factor domains, as well as the C-terminal AUX/IAA domain (with III-IV motifs) and two motifs with QSL-rich regions (**Supplementary Figure S8**). *Pilostyles* proteins present all of these domains, except for one of two QSL-rich regions (**Supplementary Figure S8**, purple domain; **Table 2**). No motifs were found to be exclusive for Apodanthaceae, Cucurbitaceae, or Fabaceae proteins.

The *LEAFY* Gene Family

Finally, the phylogenetic reconstruction of *LEAFY* genes showed that they are retained as single copy in most species, except in *Brassica rapa, Cladrastis lutea, Cucurbita maxima, Kalanchoe laxiflora, Linum perenne, L. usitatissimum*, and *Zea mays* (**Figure 7** and **Supplementary Figure S9**). Three different variants were isolated from *Pilostyles boyacensis*. *PiboLFY1* and *PiboLFY2* were found in the PbFl and PbFr transcriptomes, whereas *PiboLFY3* was detected only in the PbE + D transcriptome. *PiboLFY2* has an additional exon of 135 nt in comparison to *PiboLFY1*. *PiboLFY3* is a partial sequence that differs in two nucleotides located in the 5′UTR (**Supplementary Figure S10**).

The *LFY* variants from *Pilostyles boyacensis* cluster with the single copy found in *P. thurberi* (*PithLFY*, BS/PP, 100/1, **Figure 7**). Interestingly, the ML analysis shows *Pilostyles* homologs as closely related to Euphorbiaceae and Salicaceae genes (BS:38, **Supplementary Figure S9**), whereas in the BI

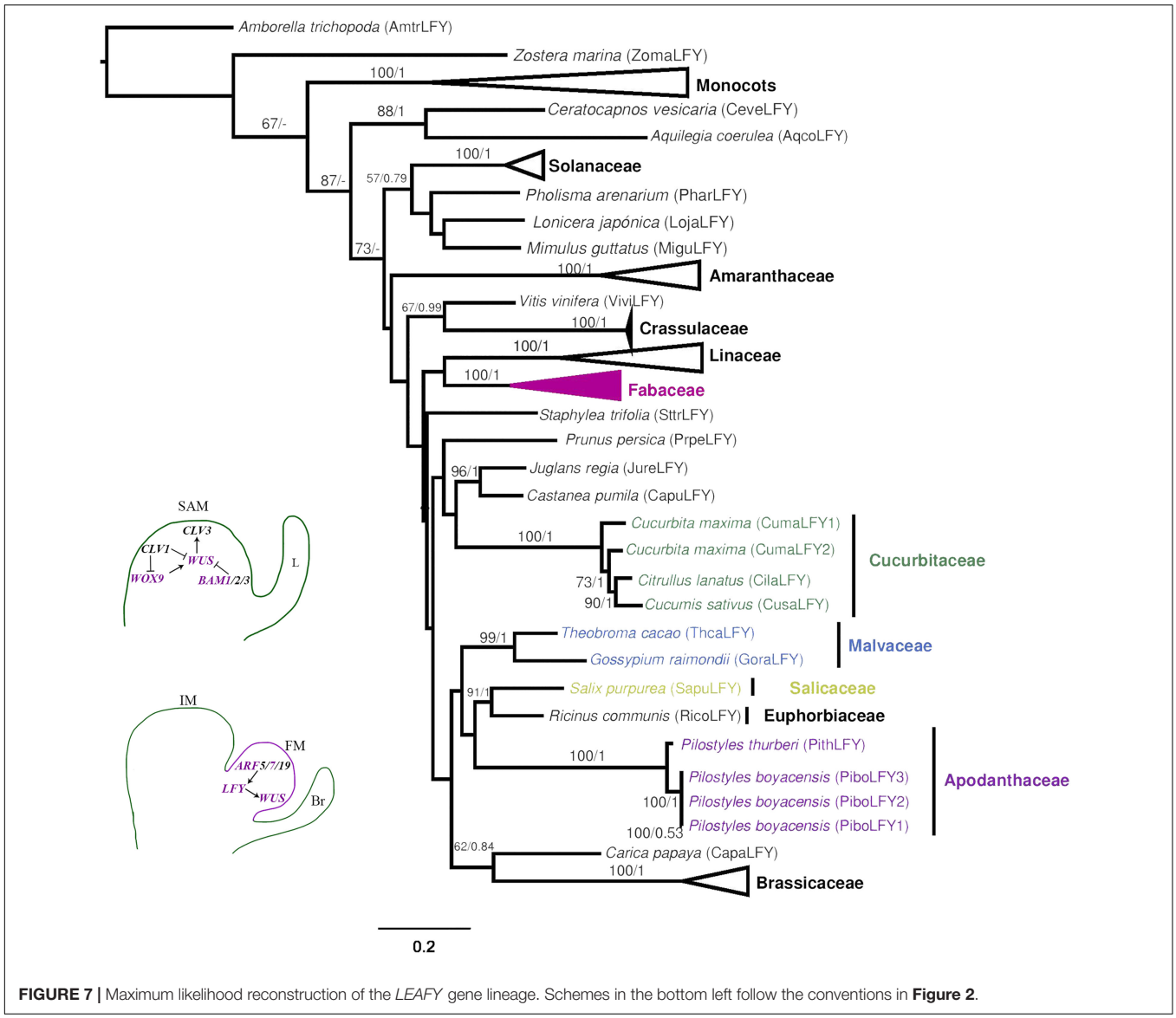

FIGURE 7 | Maximum likelihood reconstruction of the *LEAFY* gene lineage. Schemes in the bottom left follow the conventions in **Figure 2**.

analysis, they cluster with Cucurbitaceae homologs (PP: 0.78, **Supplementary Figure S9**). The MEME analysis detects the highly conserved N-terminal Floricaula/Leafy protein SAM domain and the C-terminal DNA Binding Domain Leafy/F. Additionally, an N-terminal LPPP and a GLSEE motif were detected in the full and the reduced datasets (**Supplementary Figure 10**). Sequences from *Pilostyles* showed all of these domains and motifs, except for the variant *PiboLFY3*, which is an incomplete CDS (**Table 2**). No motifs are exclusive for Apodanthaceae or Cucurbitales sequences.

DISCUSSION

Unlike the typical vegetative SAM to IM to FM developmental sequence that occurs in most angiosperms including Arabidopsis (Ó'Maoiléidigh et al., 2014), the transit to FMs in *Pilostyles* takes place directly from non-specialized endophytic tissue without recognizable vegetative or IMs (Amaral, 2007; González and Pabón-Mora, 2017). Five out of the 11 *A. thaliana* canonical gene families responsible for SAM maintenance and floral fate determinacy targeted in this study were found in *Pilostyles boyacensis*.

The *WUSCHEL* and *WUSCHEL*-Related Homeobox 9 Gene Subfamilies

The *WUSCHEL-related* homologs are represented in *Pilostyles boyacensis* by *PiboWUS*, and *PiboWOX9*. *WOX9* homologs have key roles in early embryo patterning, as well as pluripotency and cell proliferation in the SAM across seed plants (Haecker et al., 2004; Nardmann et al., 2007; Palovaara et al., 2010; Skylar et al., 2010; Zhou et al., 2018). In addition, *WOX9* homologs also play roles in inflorescence architecture and floral identity in petunia and tomato as well as in carpel development in *Arabidopsis*, and possibly in sex determination

in *Cucumis* (Wu et al., 2005; Rebocho et al., 2008; Costanzo et al., 2014; Pawełkowicz et al., 2019). *PiboWOX9* transcripts were found in all three transcriptomes including both early and late developmental stages. Based on the putative roles previously identified in model taxa, we hypothesize that *PiboWOX9* variants have pleiotropic roles in inflorescence architecture, floral identity, carpel development, and perhaps sex determination because they were found in the PbE + D and PbFl transcriptomes. Additionally, *PiboW9_2* could be involved in early embryo patterning because it was found in the PbFr transcriptome. Finally, because their protein sequences have a complete N-terminal motif MASSN and two C-terminal motifs VFIN and LQxG WOX8 (Deveaux et al., 2008; Palovaara et al., 2010), at least the PiboWOX9_2 and PiboWOX9_3 isoforms are fully functional.

PiboWUS variants were isolated exclusively from the PbFl transcriptome. Most *WUS* homologs functionally analyzed control stem cell maintenance in the SAM, the RAM, and the FMs (Laux et al., 1996). Additionally, *WUS* genes are involved in embryo patterning, leaf, perianth, anther, and ovule development (van der Graaff et al., 2009; Tsuda and Hake, 2016; Wu et al., 2019). At least PiboWUS_2 contains the TLxLFP WUS-box and the EAR-like LELxL motif; the latter is crucial in stem cell maintenance because it mediates the repression of target genes (Kieffer et al., 2006; Tsuda and Hake, 2016). Considering that SAMs in *P. boyacensis* are lacking and that *PiboWUS* homologs were not found in the PbE + D or the PbFr transcriptomes, we hypothesize that their functions are restricted to the stem cell maintenance in FMs and perhaps in anther and ovule development.

The LEUCINE-RICH REPEAT RECEPTOR-LIKE KINASE IX—A Subfamily

The LRR-RLK-IX, a subfamily in *Pilostyles*, is represented by *BAM1/2* homologs while *CLAVATA1* homologs are absent. Two copies of *BAM1/2* homologs were detected in each of the two species of *Pilostyles* sampled. The copies are found in different transcriptomes, with *PiboBAM1* active in PbE + D and PbFr, and *PiboBAM2* active in PbFl and PbFr. At least one variant of each copy conserves the extracellular leucine-rich repeat domain, necessary for detection of CLE ligands, as well as the cytoplasmic kinase domains in charge of phosphorylation of target proteins (**Supplementary Figure S6**; Hazak and Hardtke, 2016; Wu et al., 2018).

Four different functions have been assigned to *CLV1*/*BAM* genes in *A. thaliana*. The first is related to the role of *CLV3,* which binds *CLV1/2* to repress *WUSCHEL* related genes in the SAM in order to control cell differentiation and organogenesis (Fletcher, 1999; DeYoung et al., 2006; DeYoung and Clark, 2008; Hazak and Hardtke, 2016; Pan et al., 2016). *CLV1* is reinforced by *BAM* homologs as they sequester CLE ligands secreted in the periphery, resulting in the maintenance of pluripotency in the meristematic field (DeYoung and Clark, 2008). The second, involves *BAM1* in the quiescent center of the RAM restricting cell proliferation (DeYoung et al., 2006). The third role involves *BAM1/2* in the sporogenous cell fate in the anthers and in ovule development (DeYoung et al., 2006; Li et al., 2016). The fourth role is the control of vascular development in roots, shoots, and leaves by *BAM3* (Hazak and Hardtke, 2016).

BAM1/2 transcripts from PbFr lack the kinase domain and have premature stop codons (**Table 2** and **Supplementary Figure S6**). It is likely that such incomplete proteins no longer play a role in early embryogenesis, including putative plumule and radicle differentiation. This is further supported by the fact that *CLV1* homologs were not found in any of the *Pilostyles* transcriptomes, and members of the CLE family (*CLV3*) identified were assigned by similarity to the host *Dalea cuatrecasasii*. The isolation of complete BAM1/2 proteins from the PbE + D and the PbFr transcriptomes strongly suggests that the primary role of *BAM1/2* in *Pilostyles* is restricted to anther and ovule development. Nonetheless, a secondary role related to the vascular development of the floral extensor in *Pilostyles* (Amaral, 2007; González and Pabón-Mora, 2017) cannot be ruled out.

The AUXIN RESPONSE FACTOR 5/7/19 Subclade

The *ARF5/7/19* subclade in *Pilostyles* is represented only by *ARF7E* orthologs. Specifically, *PiboARF7E_2* was found in all three transcriptomes, whereas *PiboARF7E_1* was detected only in the PbFl, and *PiboARF7E_3*, *PiboARF7E_4* were found only in the PbFr transcriptome. Transcripts from *Pilostyles* (except *PiboARFE7_1*) carry intact DNA binding domains as well as AUX/IAA and auxin response factor domains. However, only one out of the two characteristic QSL-rich regions is present in all *Pilostyles* ARF7E proteins. Both, the AUX/IAA domain and the QSL region have been involved in dimerization with other ARFs (Korasick et al., 2014; Chandler, 2016). Thus, sequence analyses indicate that at least three isoforms of *PiboARF7* are fully functional. Nevertheless, the lack of *ARF7E* orthologs in *A. thaliana* hinders a direct functional comparison with *Pilostyles* homologs. Other *ARF5/7/19* are known to play redundant roles in lateral root formation, shoot regeneration, leaf polarity and expansion, FM determination, fertilization, fruit development, senescence, and organ abscission (Chandler, 2016). Altogether, our data suggests that the most likely functions of the *PiboARF7* homologs include FM determination, fertilization, and fruit development. It is possible that *PiboARF7E* genes are taking on the function of *ARF5* in activating *LFY*.

The *LEAFY* Gene Family

LFY homologs in *Pilostyles* species are present as single copy genes, even though in *P. boyacensis* three variants were isolated. *PiboLFY1* and *PiboLFY2* are present in the PbFl and PbFr transcriptomes, while *PiboLFY3* is active in the PbE + D transcriptome. The canonical C-terminal DNA binding and N-terminal FLORICAULA/LEAFY domains reported for *LFY* (Maizel et al., 2005) are conserved in two of the three *PiboLFY* variants, suggesting that they are functional. *LFY* is an indirect

target of *FLOWERING LOCUS T* (*FT*), the florigen, and is a master regulator of FM fate because it represses IM identity and promotes floral organ identity genes (Moyroud et al., 2010). Our results point to conserved roles of *PiboLFY* genes in establishing FM identity and perhaps together with other cofactors activating floral organ identity in *Pilostyles*.

CONCLUSION

The endoparasitic lifestyle of Apodanthaceae is accompanied by a direct transition from a highly reduced endophyte to FMs. We used comparative transcriptomics from three developmental stages of *Pilostyles boyacensis* with and without the host tissues to investigate the genetic regulatory networks involved in SAM and FM identity and maintenance. Eleven canonical gene families responsible for SAM maintenance and floral fate determinacy were targeted in this study. Only five of them were found in *Pilostyles*, namely *ARF7, BAM1, LFY, WOX9*, and *WUS*. No orthologs of *ARF5, ARF19, BAM2, BAM3, CLV1,* or *CLV3* were found. The lack of SAMs and leaves seems to correlate with reductions in the number of genes for the most important gene families controlling the fine-tuning between pluripotency and organogenesis during vegetative growth. Most genes retained are likely to be functioning in establishing reproductive transition and FM fate, as well as early embryogenesis. We provide the first comprehensive comparative platform to assess meristematic activity in the reduced vegetative parts of an endo-holoparasitic plant.

DATA AVAILABILITY STATEMENT

The datasets presented in this study can be found in online repositories. The names of the repository/repositories and accession number(s) can be found below: NCBI GenBank under accession numbers MN946521–MN946537. Alignments used are in **Supplementary Material S11**.

AUTHOR CONTRIBUTIONS

AG, NP-M, and FG conceived and designed the research and performed field and lab procedures, as well as gene evolution analyses. JA performed the assembly and BLAST analyses. All authors wrote, revised, and approved the submitted version.

FUNDING

This project was supported by the Universidad Nacional de Colombia, Vicerrectoría de Investigaciones through the Convocatoria Nacional de Proyectos para el Fortalecimiento de la Investigación, Creación e Innovación de la Universidad Nacional De Colombia 2016–2018, project number 37247, and by Universidad de Antioquia, Estrategia de Sostenibilidad 2018–2019 and Convocatoria Programáticas 2017-16302 grants.

ACKNOWLEDGMENTS

We thank the students Sebastián Guzmán and Paola Piñeros (Universidad Nacional de Colombia) for field work support. We also thank Sebastian González (Massachusetts College of Art and Design) for taking the photographs in **Figure 1**. Preliminary results from this research were presented in the IX Latin American Society for Developmental Biology Meeting (Medellín, Colombia, 2017).

SUPPLEMENTARY MATERIAL

The Supplementary Material for this article can be found online at: https://www.frontiersin.org/articles/10.3389/fevo.2020.00209/full#supplementary-material

REFERENCES

Afgan, E., Baker, D., Batut, B., van den Beek, M., Bouvier, D., Čech, M., et al. (2018). The Galaxy platform for accessible, reproducible and collaborative biomedical analyses: 2018 update. *Nucleic Acids Res.* 46, W537–W544. doi: 10.1093/nar/gky379

Amaral, M. M. (2007). *A estrutura da angiosperma endoparasita Pilostyles ulei (Apodanthaceae): Interface e impacto no lenho de Mimosa spp*. Available online at: http://www.teses.usp.br/teses/disponiveis/41/41132/tde-05112007-095018/ (accessed March 11, 2017).

Amaral, M. M., and Ceccantini, G. (2011). The endoparasite *Pilostyles ulei* (Apodanthaceae – Cucurbitales) influences wood structure in three host species of Mimosa. *IAWA J.* 32, 1–13. doi: 10.1163/22941932-90000038

Arias-Agudelo, L. M., González, F., Isaza, J. P., Alzate, J. F., and Pabón-Mora, N. (2019). Plastome reduction and gene content in New World *Pilostyles* (Apodanthaceae) unveils high similarities to African and Australian congeners. *Mol. Phylogenet. Evol.* 135, 193–202. doi: 10.1016/j.ympev.2019.03.014

Bellot, S., and Renner, S. S. (2014). The systematics of the worldwide endoparasite family Apodanthaceae (Cucurbitales), with a key, a map, and color photos of most species. *PhytoKeys* 36, 41–57. doi: 10.3897/phytokeys.36.7385

Blarer, A., Nickrent, D. L., and Endress, P. K. (2004). Comparative floral structure and systematics in Apodanthaceae (Rafflesiales). *Plant Syst. Evol.* 245, 119–142. doi: 10.1007/s00606-003-0090-2

Brasil, B. D. A. (2010). *Ciclo de Vida, Fenologia e Anatomia Floral de Pilostyles (Apodanthaceae - Rafflesiaceae s.l.): Subsídios Para um Posicionamento Filogenético da Família Apodanthaceae*. Available online at: http://www.teses.usp.br/teses/disponiveis/41/41132/tde-10122010-105707/ (accessed March 11, 2017).

Bryan, A. C., Obaidi, A., Wierzba, M., and Tax, F. E. (2012). XYLEM INTERMIXED WITH PHLOEM1, a leucine-rich repeat receptor-like kinase required for stem growth and vascular development in *Arabidopsis thaliana*. *Planta* 235, 111–122. doi: 10.1007/s00425-011-1489-6

Chandler, J. W. (2016). Auxin response factors. *Plant Cell Environ.* 39, 1014–1028. doi: 10.1111/pce.12662

Chandler, J. W., and Werr, W. (2015). Cytokinin–auxin crosstalk in cell type specification. *Trends Plant Sci.* 20, 291–300. doi: 10.1016/j.tplants.2015.02.003

Costanzo, E., Trehin, C., and Vandenbussche, M. (2014). The role of WOX genes in flower development. *Ann. Bot.* 114, 1545–1553. doi: 10.1093/aob/mcu123

Darriba, D., Posada, D., Kozlov, A. M., Stamatakis, A., Morel, B., and Flouri, T. (2019). ModelTest-NG: a new and scalable tool for the selection of DNA and protein evolutionary models. *Mol. Biol. Evol.* 37, 291–294. doi: 10.1093/molbev/msz189

Denay, G., Chahtane, H., Tichtinsky, G., and Parcy, F. (2017). A flower is born: an update on *Arabidopsis* floral meristem formation. *Curr. Opin. Plant Biol.* 35, 15–22. doi: 10.1016/j.pbi.2016.09.003

Deveaux, Y., Toffano-Nioche, C., Claisse, G., Thareau, V., Morin, H., Laufs, P., et al. (2008). Genes of the most conserved WOX clade in plants affect root and flower development in *Arabidopsis*. *BMC Evol. Biol.* 8:291. doi: 10.1186/1471-2148-8-291

DeYoung, B. J., Bickle, K. L., Schrage, K. J., Muskett, P., Patel, K., and Clark, S. E. (2006). The CLAVATA1-related BAM1, BAM2 and BAM3 receptor kinase-like proteins are required for meristem function in *Arabidopsis*: BAM receptor kinases regulate meristem function. *Plant J.* 45, 1–16. doi: 10.1111/j.1365-313X.2005.02592.x

DeYoung, B. J., and Clark, S. E. (2008). BAM receptors regulate stem cell specification and organ development through complex interactions with CLAVATA signaling. *Genetics* 180, 895–904. doi: 10.1534/genetics.108.091108

Finet, C., Berne-Dedieu, A., Scutt, C. P., and Marlétaz, F. (2013). Evolution of the ARF gene family in land plants: old domains, new tricks. *Mol. Biol. Evol.* 30, 45–56. doi: 10.1093/molbev/mss220

Fletcher, J. C. (1999). Signaling of cell fate decisions by CLAVATA3 in *Arabidopsis* shoot meristems. *Science* 283, 1911–1914. doi: 10.1126/science.283.5409.1911

Gaillochet, C., and Lohmann, J. U. (2015). The never-ending story: from pluripotency to plant developmental plasticity. *Development* 142, 2237–2249. doi: 10.1242/dev.117614

González, F., and Pabón-Mora, N. (2014a). First reports and generic descriptions of the achlorophyllous holoparasites Apodanthaceae (Cucurbitales) of Colombia. *Actualidades Biol.* 36, 123–135.

González, F., and Pabón-Mora, N. (2014b). *Pilostyles boyacensis* a new species of Apodanthaceae (Cucurbitales) from Colombia. *Phytotaxa* 178:138. doi: 10.11646/phytotaxa.178.2.5

González, F., and Pabón-Mora, N. (2017). Floral development and morphoanatomy in the holoparasitic *Pilostyles boyacensis* (Apodanthaceae, Cucurbitales) reveal chimeric half-staminate and half-carpellate flowers. *Int. J. Plant Sci.* 178, 522–536. doi: 10.1086/692505

Goodstein, D. M., Shu, S., Howson, R., Neupane, R., Hayes, R. D., Fazo, J., et al. (2012). Phytozome: a comparative platform for green plant genomics. *Nucleic Acids Res.* 40, D1178–D1186. doi: 10.1093/nar/gkr944

Grabherr, M. G., Haas, B. J., Yassour, M., Levin, J. Z., Thompson, D. A., Amit, I., et al. (2011). Full-length transcriptome assembly from RNA-Seq data without a reference genome. *Nat. Biotechnol.* 29, 644–652. doi: 10.1038/nbt.1883

Ha, C. M., Jun, J. H., and Fletcher, J. C. (2010). "Chapter Four - Shoot Apical Meristem Form and Function," in *Current Topics in Developmental Biology Plant Development*, ed. M. C. P. Timmermans (Cambridge, MA: Academic Press), 103–140. doi: 10.1016/s0070-2153(10)91004-1

Haecker, A., Gross-Hardt, R., Geiges, B., Sarkar, A., Breuninger, H., Herrmann, M., et al. (2004). Expression dynamics of WOX genes mark cell fate decisions during early embryonic patterning in *Arabidopsis thaliana*. *Development* 131, 657–668. doi: 10.1242/dev.00963

Hall, T. A. (1999). BioEdit: a user-friendly biological sequence alignment editor and analysis program for Windows 95/98/NT. *Nucleic Acids Symp. Ser.* 41, 95–98.

Hardtke, C. S., Ckurshumova, W., Vidaurre, D. P., Singh, S. A., Stamatiou, G., Tiwari, S. B., et al. (2004). Overlapping and non-redundant functions of the *Arabidopsis* auxin response factors MONOPTEROS and NONPHOTOTROPIC HYPOCOTYL 4. *Development* 131, 1089–1100. doi: 10.1242/dev.00925

Hazak, O., and Hardtke, C. S. (2016). CLAVATA 1-type receptors in plant development. *EXBOTJ* 67, 4827–4833. doi: 10.1093/jxb/erw247

Heide-Jørgensen, H. (2008). *Parasitic Flowering Plants*. Boston: Brill.

Katoh, K., and Standley, D. M. (2013). MAFFT multiple sequence alignment software version 7: improvements in performance and usability. *Mol. Biol. Evol.* 30, 772–780. doi: 10.1093/molbev/mst010

Kieffer, M., Stern, Y., Cook, H., Clerici, E., Maulbetsch, C., Laux, T., et al. (2006). Analysis of the transcription factor WUSCHEL and its functional homologue in *Antirrhinum* reveals a potential mechanism for their roles in meristem maintenance. *Plant Cell* 18, 560–573. doi: 10.1105/tpc.105.039107

Korasick, D. A., Westfall, C. S., Lee, S. G., Nanao, M. H., Dumas, R., Hagen, G., et al. (2014). Molecular basis for AUXIN RESPONSE FACTOR protein interaction and the control of auxin response repression. *Proc. Natl. Acad. Sci. U.S.A.* 111, 5427–5432. doi: 10.1073/pnas.1400074111

Laux, T., Mayer, K. F., Berger, J., and Jürgens, G. (1996). The WUSCHEL gene is required for shoot and floral meristem integrity in *Arabidopsis*. *Development* 122, 87–96.

Li, H., Shi, Q., Zhang, Z.-B., Zeng, L.-P., Qi, J., and Ma, H. (2016). Evolution of the leucine-rich repeat receptor-like protein kinase gene family: ancestral copy number and functional divergence of BAM1 and BAM2 in Brassicaceae: evolution of the LRR-RLK gene family. *J. Syt. Evol.* 54, 204–218. doi: 10.1111/jse.12206

Maizel, A., Busch, M. A., Tanahashi, T., Perkovic, J., Kato, M., Hasebe, M., et al. (2005). The floral regulator LEAFY evolves by substitutions in the DNA binding domain. *Science* 308, 260–263. doi: 10.1126/science.1108229

Matasci, N., Hung, L.-H., Yan, Z., Carpenter, E. J., Wickett, N. J., Mirarab, S., et al. (2014). Data access for the 1,000 Plants (1KP) project. *Gigascience* 3:17. doi: 10.1186/2047-217X-3-17

Miller, M. A., Pfeiffer, W., and Schwartz, T. (2010). "Creating the CIPRES Science Gateway for inference of large phylogenetic trees," in *Proceedings of the Gateway Computing Environments Workshop (GCE)*, (New Orleans, LA: IEEE), 1–8.

Moyroud, E., Kusters, E., Monniaux, M., Koes, R., and Parcy, F. (2010). LEAFY blossoms. *Trends Plant Sci.* 15, 346–352. doi: 10.1016/j.tplants.2010.03.007

Nardmann, J., Zimmermann, R., Durantini, D., Kranz, E., and Werr, W. (2007). WOX gene phylogeny in Poaceae: a comparative approach addressing leaf and embryo development. *Mol. Biol. Evol.* 24, 2474–2484. doi: 10.1093/molbev/msm182

Nickrent, D. L. (2020). Parasitic angiosperms: How often and how many? *TAXON* 69, 5–27. doi: 10.1002/tax.12195

Nikolov, L. A., Endress, P. K., Sugumaran, M., Sasirat, S., Vessabutr, S., Kramer, E. M., et al. (2013). Developmental origins of the world's largest flowers, Rafflesiaceae. *PNAS* 110, 18578–18583. doi: 10.1073/pnas.1310356110

Ó'Maoiléidigh, D. S., Graciet, E., and Wellmer, F. (2014). Gene networks controlling *Arabidopsis thaliana* flower development. *New Phytol.* 201, 16–30. doi: 10.1111/nph.12444

Pabón-Mora, N., Ambrose, B. A., and Litt, A. (2012). Poppy APETALA1/FRUITFULL orthologs control flowering time, branching, perianth identity, and fruit development. *Plant Physiol.* 158, 1685–1704. doi: 10.1104/pp.111.192104

Palovaara, J., Hallberg, H., Stasolla, C., and Hakman, I. (2010). Comparative expression pattern analysis of WUSCHEL-related homeobox 2 (WOX2) and WOX8/9 in developing seeds and somatic embryos of the gymnosperm *Picea abies*. *New Phytol.* 188, 122–135. doi: 10.1111/j.1469-8137.2010.03336.x

Pan, L., Lv, S., Yang, N., Lv, Y., Liu, Z., Wu, J., et al. (2016). The multifunction of CLAVATA2 in plant development and immunity. *Front. Plant Sci.* 7:1573. doi: 10.3389/fpls.2016.01573

Pawełkowicz, M., Pryszcz, L., Skarzyńska, A., Wóycicki, R. K., Posyniak, K., Rymuszka, J., et al. (2019). Comparative transcriptome analysis reveals new molecular pathways for cucumber genes related to sex determination. *Plant Reprod.* 32, 193–216. doi: 10.1007/s00497-019-00362-z

Poole, R. L. (2007). The TAIR database. *Methods Mol. Biol.* 406, 179–212. doi: 10.1007/978-1-59745-535-0_8

Rambaut, A. (2006). *FigTree Tree Figure Drawing Toll version 1.3.1. Institute of Evolutionary Biology, University of Edinburgh.* Available online at: http://tree.bio.ed.ac.uk/software/figtree/ (accessed January 31, 2013).

Rebocho, A. B., Bliek, M., Kusters, E., Castel, R., Procissi, A., Roobeek, I., et al. (2008). Role of EVERGREEN in the development of the cymose petunia inflorescence. *Dev. Cell* 15, 437–447. doi: 10.1016/j.devcel.2008.08.007

Ronquist, F., Teslenko, M., van der Mark, P., Ayres, D. L., Darling, A., Höhna, S., et al. (2012). MrBayes 3.2: efficient Bayesian phylogenetic inference and model choice across a large model space. *Syst. Biol.* 61, 539–542. doi: 10.1093/sysbio/sys029

Rutherford, R. J. (1970). The anatomy and cytology of *Pilostyles thurberi* Gray (Rafflesiaceae). *Aliso* 7, 263–288. doi: 10.5642/aliso.19700702.13

Skylar, A., Hong, F., Chory, J., Weigel, D., and Wu, X. (2010). STIMPY mediates cytokinin signaling during shoot meristem establishment in *Arabidopsis* seedlings. *Development* 137, 541–549. doi: 10.1242/dev.041426

Stamatakis, A., Hoover, P., and Rougemont, J. (2008). A rapid bootstrap algorithm for the RAxML web servers. *Syst. Biol.* 57, 758–771. doi: 10.1080/10635150802429642

Taylor-Teeples, M., Lanctot, A., and Nemhauser, J. L. (2016). As above, so below: auxin's role in lateral organ development. *Dev. Biol.* 419, 156–164. doi: 10.1016/j.ydbio.2016.03.020

Tsuda, K., and Hake, S. (2016). "Homeobox transcription factors and the regulation of meristem development and maintenance," in *Plant Transcription Factors*, ed. D. H. Gonzalez (Amsterdam: Elsevier), 215–228. doi: 10.1016/b978-0-12-800854-6.00014-2

van der Graaff, E., Laux, T., and Rensing, S. A. (2009). The WUS homeobox-containing (WOX) protein family. *Genome Biol.* 10:248. doi: 10.1186/gb-2009-10-12-248

Wagner, D., Sablowski, R. W., and Meyerowitz, E. M. (1999). Transcriptional activation of APETALA1 by LEAFY. *Science* 285, 582–584. doi: 10.1126/science.285.5427.582

Wils, C. R., and Kaufmann, K. (2017). Gene-regulatory networks controlling inflorescence and flower development in *Arabidopsis thaliana*. *Biochim. Biophys. Acta Gene Regul. Mech.* 1860, 95–105. doi: 10.1016/j.bbagrm.2016.07.014

Wu, C.-C., Li, F.-W., and Kramer, E. M. (2019). Large-scale phylogenomic analysis suggests three ancient superclades of the WUSCHEL-RELATED HOMEOBOX transcription factor family in plants. *PLoS One* 14:e0223521. doi: 10.1371/journal.pone.0223521

Wu, Q., Xu, F., and Jackson, D. (2018). All together now, a magical mystery tour of the maize shoot meristem. *Curr. Opin. Plant Biol.* 45, 26–35. doi: 10.1016/j.pbi.2018.04.010

Wu, X., Dabi, T., and Weigel, D. (2005). Requirement of homeobox gene STIMPY/WOX9 for *Arabidopsis* meristem growth and maintenance. *Curr. Biol.* 15, 436–440. doi: 10.1016/j.cub.2004.12.079

Yamaguchi, N., Wu, M.-F., Winter, C. M., Berns, M. C., Nole-Wilson, S., Yamaguchi, A., et al. (2013). A molecular framework for auxin-mediated initiation of flower primordia. *Dev. Cell* 24, 271–282. doi: 10.1016/j.devcel.2012.12.017

Zheng, Y., Wu, S., Bai, Y., Sun, H., Jiao, C., Guo, S., et al. (2019). Cucurbit Genomics Database (CuGenDB): a central portal for comparative and functional genomics of cucurbit crops. *Nucleic Acids Res.* 47, D1128–D1136. doi: 10.1093/nar/gky944

Zhou, X., Guo, Y., Zhao, P., and Sun, M. (2018). Comparative analysis of WUSCHEL-related homeobox genes revealed their parent-of-origin and cell type-specific expression pattern during early embryogenesis in tobacco. *Front. Plant Sci.* 9:311. doi: 10.3389/fpls.2018.00311

Conflict of Interest: The authors declare that the research was conducted in the absence of any commercial or financial relationships that could be construed as a potential conflict of interest.